Sex Plant Reprod (1995) 8:197–204

ORIGINAL PAPER

T. N. Naumova · M. T. M. Willemse

Ultrastructural characterization of apospory in *Panicum maximum*

Received: 19 October 1994 / Revision accepted: 29 March 1995

Abstract The nucellar ultrastructure of apomictic *Panicum maximum* was analyzed during the meiocytic stage and during aposporous embryo sac formation. At pachytene the megameiocyte shows a random cell organelle distribution and sometimes only an incomplete micropylar callose wall. The chalazal nucellar cells are meristematic until the tetrad stage. They can turn into initial cells of aposporous embryo sacs. The aposporous initials can be recognized by their increased cell size, large nucleus, and the presence of many vesicles. The cell wall is thin with few plasmodesmata. If only a sexual embryo sac is formed, the nucellar cells retain their meristematic character. The aposporous initial cell is somewhat comparable to a vacuolated functional megaspore. It shows large vacuoles around the central nucleus and is surrounded by a thick cell wall without plasmodesmata. In the mature aposporous embryo sac the structure of the cells of the egg apparatus is similar to each other. In the chalazal part of the egg apparatus the cell walls are thin and do not hamper the transfer of sperm cells. Structural and functional aspects of nucellar cell differentiation and aposporous and sexual embryo sac development are discussed.

Key words Apomixis · Apospory · Aposporous initial · Aposporous embryo sac · Ultrastructure · *Panicum*

Introduction

Apomixis is a characteristic feature of many grasses (Brown and Emery 1958) and leads to maternal heredity. Apospory results in an embryo sac with diploid nuclei because it originates from a diploid nucellar cell. Apospory is commonly found in many Gramineae such as *Poa*, *Panicum*, *Sorghum*, *Hierochloë*, and *Calamagrostis*. It is also found in many dicots; for example, the Rosaceae genera *Malus*, *Prunus*, *Sorbus* and the Asteraceae genera *Hieracium* and *Artemisia*. Two types of aposporous embryo sac are distinguishable: Hieracium-type and Panicum-type (Battaglia 1963; Rutishauser 1969).

Panicum-type apospory was first observed in *Panicum maximum* (Warmke 1954). The apospore develops to a diploid, monopolar four-nucleate embryo sac with a three-celled egg apparatus and a central cell with one nucleus. The chromosome number of a diploid embryo sac nucleus is 2n=32. This characterization of the *P. maximum* aposporic embryo sac (AE) was also confirmed by Savidan (1982). The aposporous Panicum- and meiotic Polygonum-type of embryo sacs can both develop in the nucellus, but commonly only the AE remains. In *Poa pratensis* the initial cell of an AE is characterized by dense cytoplasm and a thick cell wall (Abeln et al. 1985). This paper analyzes structural aspects of apospory in *P. maximum*, with emphasis on the origin of the aposporic initial and its development into an aposporic embryo sac.

T. N. Naumova
Komarov Botanical Institute, Prof. Popov Street 2, 197376, St. Petersburg, Russia

M. T. M. Willemse (✉)
Department of Plant Cytology and Morphology, Wageningen Agricultural University, Arboretumlaan 4, 6703 BD Wageningen, The Netherlands;
Fax: (31) 8370–85005

Materials and methods

Panicum maximum Jacq. plants were cultivated in a greenhouse of the Wageningen Agricultural University (The Netherlands). J.H. Savidan kindly supplied the apomictic KK-15 and sexual 1-S-16, seeds which were similar to those used in a breeding program of the ORSTOM Research Centre (Montpellier, France). For this investigation the apomictic plants were used.

Ovaries of apomictic plants at early spike development were dissected and fixed in 3.5% glutaraldehyde in 0.2 M phosphate buffer (pH 7.2) for 4 h at room temperature. They were post-fixed in 2% OsO_4 in 0.2 M phosphate buffer (pH 7.8) for 12 h at 4°C. Specimens were rinsed in 0.2 M phosphate buffer, dehydrated, stained with 2% uranyl acetate in 70% ethanol for 2 h, dehydrated further in an alcohol-acetone series and embedded in Epon-araldite mixture. Ultrathin sections were cut with a diamond knife on a LKB ultramicrotome and post-stained with uranyl acetate and lead citrate. Semithin sections were stained with toluidine blue. JEM-

3000 and Hitachi-600 transmission electron microscopes were used for observations. The same procedure was used for one sexual ovule. For light microscopy studies the embryo sacs were dissected by hand from ovules without maceration and investigated with phase-contrast microscopy.

For the study of callose deposition, a 0.005% solution of aniline blue in 0.15 M K_2HPO_4 was used on 25 fresh ovaries. The ovules were released from ovaries by gentle pressure and examined with a Nikon Labophot epifluorescence microscope at 420 nm wavelength.

The nucleus/cytoplasm ratio, nucleus/nucleolus ratio and vesicles densities were determined by weighing cut photocopies of five different cells. The density of vesicles is given as a percentage of the total cell area. Ribosomes were counted in a 1 μm^2 area of cytoplasm of five cells. Cell wall measurements represent the thickness of wall between two cells.

Results

The megameiocyte and nucellar cells

At an early stage of ovule development in an apomictic plant, a hypodermal nucellar cell enlarges and becomes a megameiocyte (MMC) (Fig. 1). The area ratio of cytoplasm to nucleus of the MMC is approximately 4:1, and that of nucleus to nucleolus is 20:1. The centrally positioned nucleus is large and irregular in shape. The number of ribosomes is about 57/μm^2 cytoplasm. Single- and multiple-membrane structures enclosing cytoplasm that contains ribosomes are observed (Fig. 2). The thickness of the MMC cell wall (without plasmodesmata) at the micropylar side is about 0.3 μm and that of the chalazal wall (with plasmodesmata) bordering the nucellus is about 0.05 μm (Figs. 2, 3). In this stage aniline blue staining revealed for about 15% of the investigated apomictic ovules a callose wall deposition only as a micropylar cap of the MMC (Fig. 4). Most ovules show a complete callose wall around the MMC. Nucellar cells surrounding the MMC are all similar in their ultrastructure. The area ratio of cell cytoplasm to nucleus is approximately 3:2. The centrally positioned nucleus is large and irregular in shape. Ribosomes are abundant, about 110/μm^2 of cytoplasm. Vesicles are small and cover about 4% of the cell area. Mitochondria are uniform, oval, with well-developed cristae. Plastids are elongated or dumbbell shaped (Fig. 5). Each cell has a thin cell wall, about 0.1 μm thick, with plasmodesmata (Fig. 6).

The initial cell of the aposporous embryo sac

The dyad, tetrad or developing sexual embryo sacs very often degenerate in aposporous plants. Degeneration of all megaspores begins at the tetrad stage (Fig. 7). At the same time, the surrounding chalazal nucellar cells begin to change. Close to the degenerating structures the nucellar cells increase in volume, assume a spherical shape, and show numerous small vacuoles (Fig. 7). These nucellar cells represent the initial cells of the aposporous Panicum-type embryo sac (AI). In the AI the area ratio of cytoplasm to nucleus is 4:1 and nucleus to nucleolus is approximately 10:1. About 80 ribosomes and polysomes are present per μm^2 of cytoplasm. Small vacuoles and vesicles are numerous and cover about 25% of the cytoplasmic area. Mitochondria have well-pronounced cristae. Some plastids are elongated (Fig. 8). The cell wall is rather uniform in thickness, about 0.1 μm. Plasmodesmata are scarcely observed over long distances of the cell wall (Fig. 9). Some of them seem to be closed by cell-wall material (Fig. 10). In some ovules AIs were also observed along with a degenerating coenocyte of a sexual embryo sac (Fig. 11); these are similar to the AIs present during megaspore degeneration.

The one-nucleate and mature aposporous embryo sac

More than one aposporous embryo sac (AE) can develop in the nucellus (Fig. 12). In such an ovule these embryo sacs usually show different positions and developmental stages. Monopolarity and absence of antipodal cells are characteristic features of the aposporous Panicum-type embryo sac (Fig. 13). In a one-nucleate AE the nucleus and most of the cytoplasm are positioned in the cell center and bordered by vacuoles (Fig. 14). The area ratio of cell cytoplasm to nucleus is 6:1; that of nucleus to nucleolus is 3:2. The one-nucleated AI contains many ribosomes, about 210/μm^2 cytoplasm. Mitochondria and plastids are abundant. The cell walls of both AEs are very thick, together measuring about 0.7 μm. Plasmodesmata were not observed (Fig. 15). Degenerating nucellar cells were also observed (Figs. 11, 14).

The monopolar mature AE of *P. maximum* has four cells and no antipodals (Fig. 13). In the micropylar part of the embryo sac the cells of the egg apparatus are vacuolated. Mitochondria and small plastids were observed mainly in the micropylar part of the cells. The filiform apparatus characterizes the synergids (Fig. 16). The nuclei of synergids are situated in the center of the cell,

Fig. 1 Survey of a young ovule of an apomicyic plant with integument, nucellus and enlarged MMC at zygotene-pachytene stage. ×400. *Abbreviations* (all figures) *AE* aposporous embryo sac, *AI* initial cell of aposporic embryo sac, *CC* central cell, *CW* cell wall, *D* degeneration, *EC* egg cell, *EA* egg apparatus, *ES* sexual embryo sac, *FA* filiform apparatus, *II* inner integument, *MMC* megameiocyte, *M* mitochondria, *MM* multiple membrane structure, *N* nucleus, *n* nucleolus, *Nu* nucellus, *P* plastid, *PD* plasmodesmata, *SY* synergid, *SM* single membrane structure, *VE* vesicles, *VA* vacuoles. The unnumbered *bars* represent 1 μm. Except for Fig. 20, all figures originate from apomictic plants

Fig. 2 Cytoplasm at micropylar part of MMC with thick cell wall and multi (*MM*) or single membrane (*SM*) structures. ×16 000

Fig. 3 Cytoplasm at chalazal part of MMC with thin cell wall with plasmodesmata, bordering a chalazal nucellus cell. ×16 000

Fig. 4 Incomplete callose deposition in a cap at the micropylar part of MMC (*arrow*). ×120

Fig. 5 Chalazal nucellar cell at MMC stage. Note the dense cytoplasm with plastids, mitochondria, vesicles and ribosomes. The cell wall contains plasmodesmata. ×20 000

Fig. 6 Detail of the nucellar cell wall with plasmodesmata. Note the ribosomes. ×70 000

Fig. 9 Cell wall of an AI with a plasmodesma. ×50 000

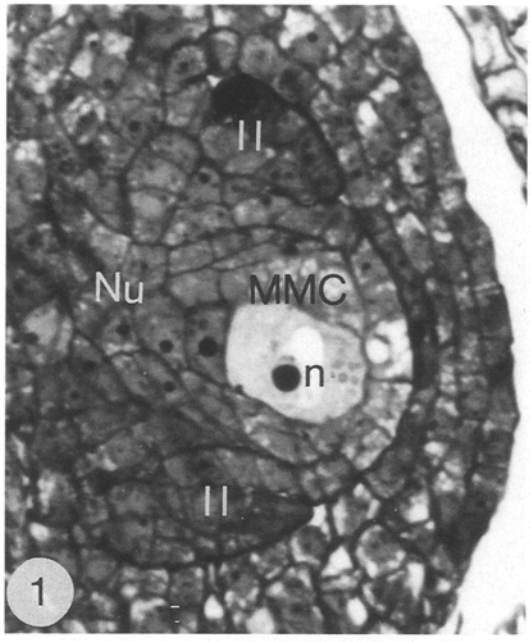
II
Nu
MMC
n
II
1

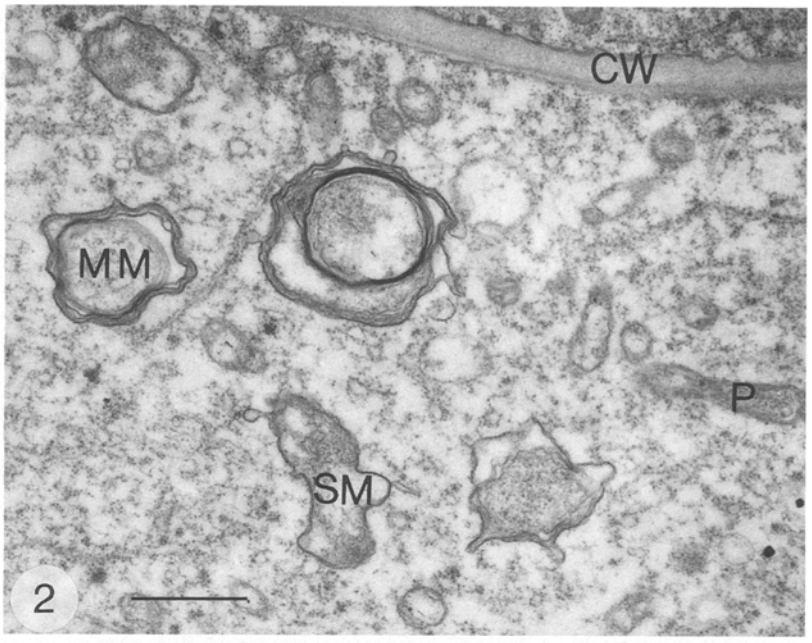
CW
MM
P
SM
2

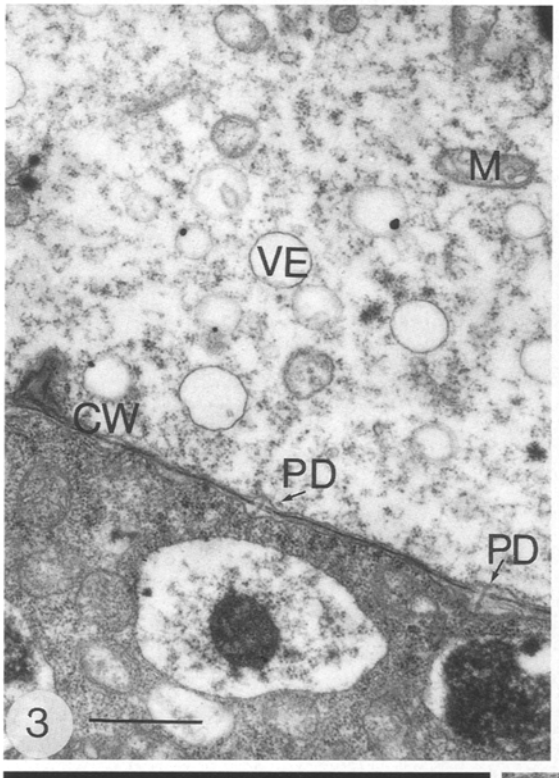
M
VE
CW
PD
PD
3

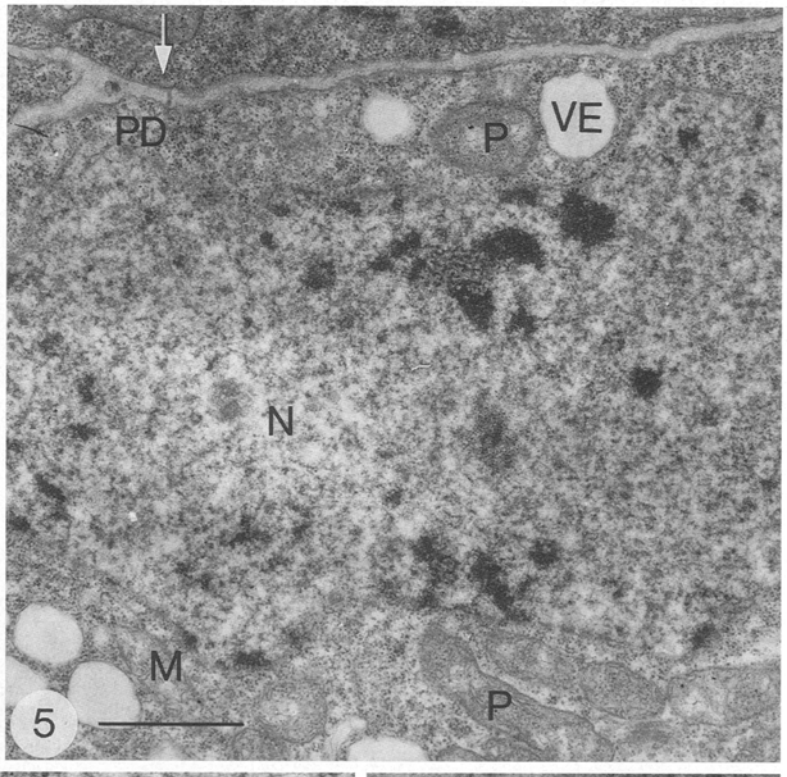
PD
P
VE
N
M
P
5

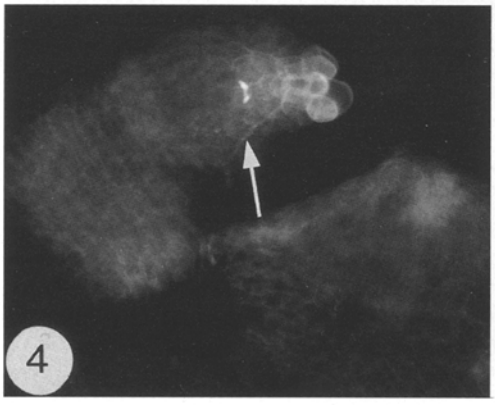
4

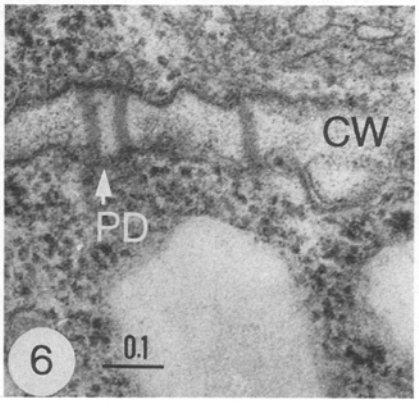
CW
PD
6
0.1

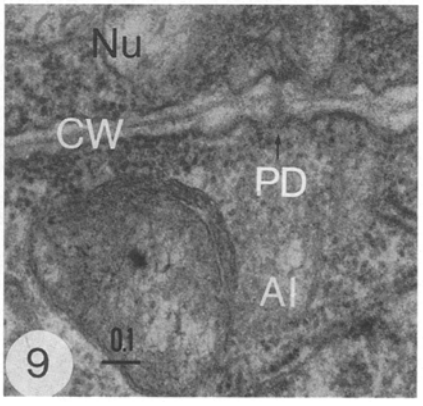
Nu
CW
PD
AI
9
0.1

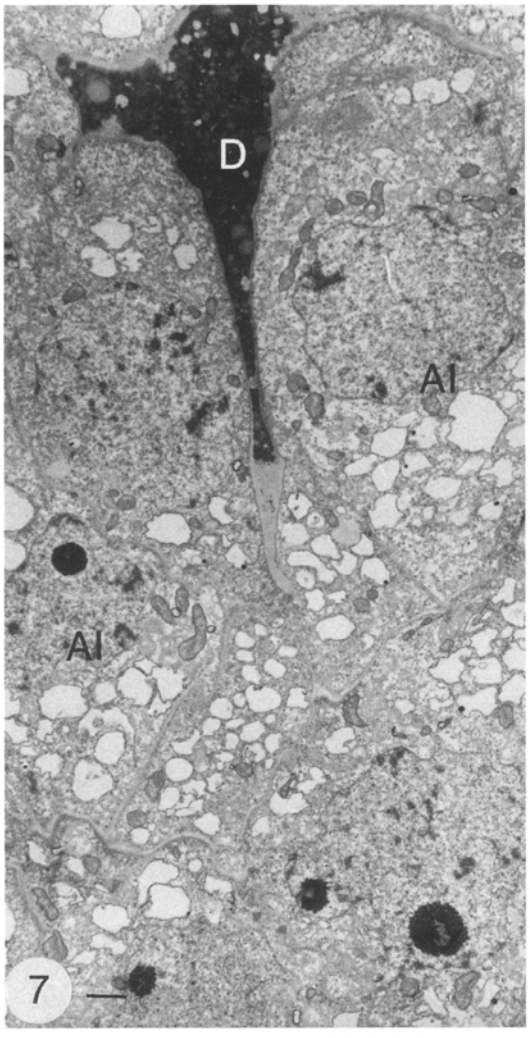
D
AI
AI
7

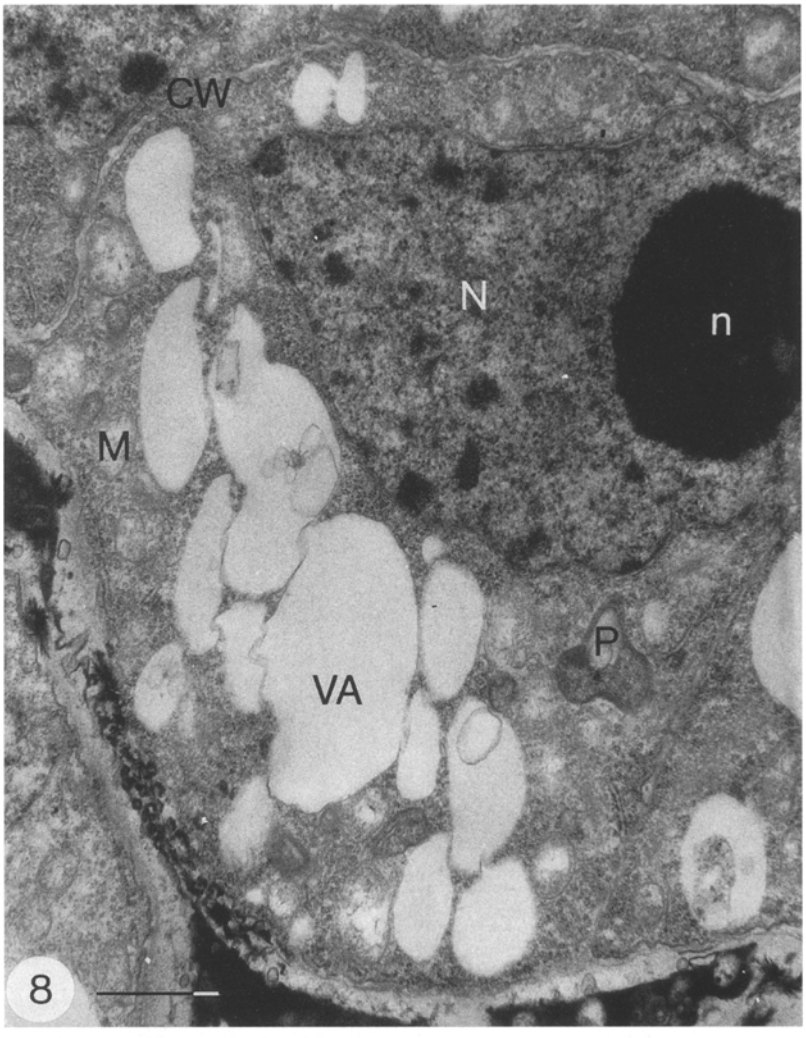
CW
N
n
M
P
VA
8

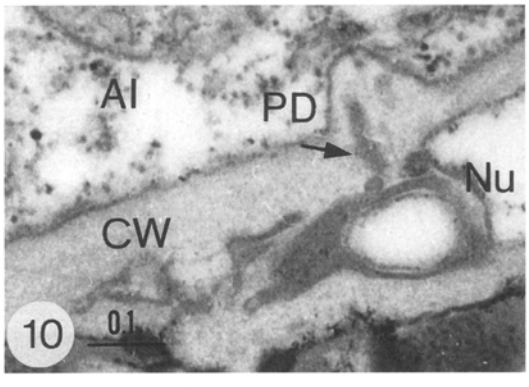
AI
PD
Nu
CW
10
01

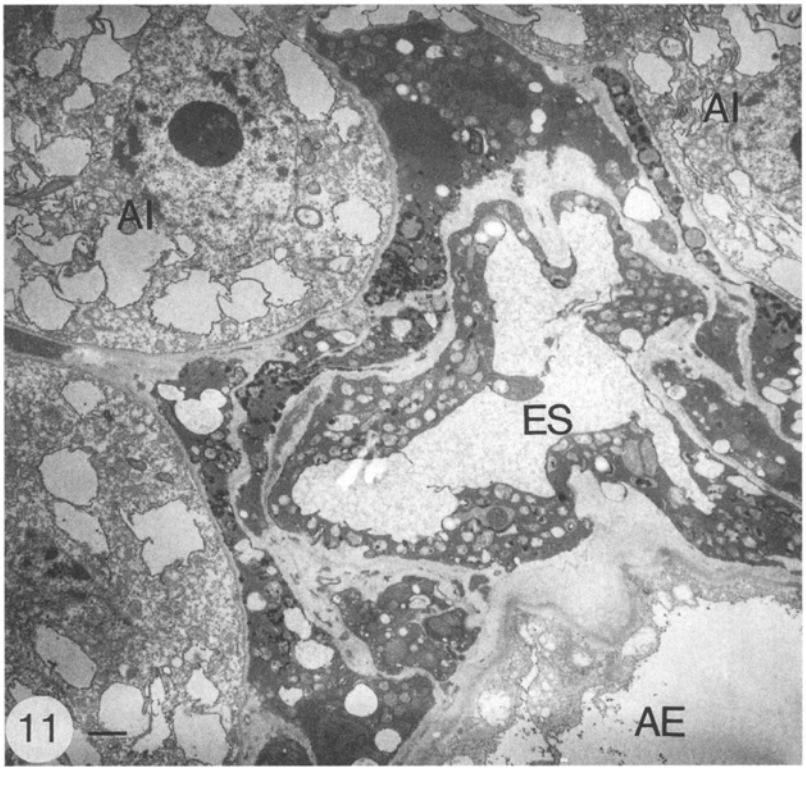
AI
AI
ES
AE
11

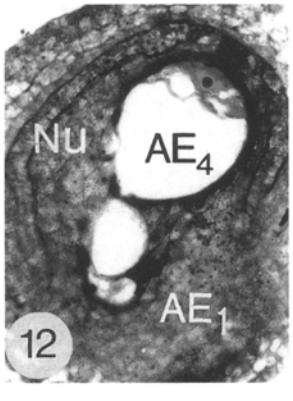
Nu
AE4
AE1
12


EA
N
CC
13

most vesicles and small vacuoles are present in the chalazal part. There is no degeneration of one of the synergids. The fine structure of the egg cell looks very similar to that of synergids. The central cell has a large vacuole, and its nucleus is positioned against the egg apparatus.

Cell walls of the egg cell and synergids show variable thickness. Close to the micropylar cell part the cell walls between the synergids are about 0.2 μm thick (Fig. 17). At the chalazal end this wall is 0.1–0.5 μm thick, and contains plasmodesmata (Fig. 18). The wall between the egg cell and the central cell is very thin, about 0.05 μm thick, or almost absent (Fig. 19).

The nucellar cells bordering the sexual coenocytic embryo sac

The normal sexual embryo sac of the Polygonum type develops in apomictic *P. maximum,* after meiosis, from the chalazal megaspore of the tetrad to a coenocyte. The cell wall of the four-nucleated coenocyte, bordering the nucellar cells, has no plasmodesmata. The nucellar cells at the chalazal part of the embryo sac are marked by dense cytoplasm, randomly localized small vesicles, and a cell wall about 0.1 μm thick with some plasmodesmata (Fig. 20).

Discussion

Ultrastructural data about apospory and other types of apomixis are very scarce and are not discussed in recent publications (Koltunow 1993). The research presented here shows that in apomictic *P. maximum* the aposporous Panicum-type embryo sac develops more frequently, and the sexual embryo sac commonly degenerates, as stated earlier (Warmke 1954). In the apomictic *P.maximum* line KK-15 the first steps of megasporogenesis are commonly present. The ultrastructure of the MMC during the zygotene/pachytene stage is comparable to that observed in *Zea* (Russell 1979) and *Capsella* (Schulz and Jensen 1981, 1986). The presence of single- or multiple-membrane structures may represent a lytic activity during the transition from sporophyte to gametophyte (Dickinson and Heslop-Harrison 1977; Dickinson 1981). In the case of *P. maximum* the multiple membrane structures also may point to a transition to a gametophytic generation.

The differences in cell-wall thickness at the micropylar and chalazal parts of the MMC can be related to the appearance of the callose only as a cap on the top of the micropylar part of the MMC. This indicates incomplete callose wall formation and cell isolation. However, in the apomictic plants the complete callose wall formation dominates. In the diplosporous *Elymus rectisetus* (Carman et al. 1991) the micropylar cell walls of the MMC were significantly thicker than those of the diplosporic MMC in a comparable stage. Such an incomplete callose deposition, as a cap on top of the MMC, was also described in aposporous *Poa pratensis* genotypes and was correlated with dyad or tetrad degeneration (Naumova et al. 1993). The incomplete callose wall in *P. maximum* is probably an early sign of low cell activity, which will be followed by degeneration of the MMC. Because of the appearance of both complete and incomplete callose in different ovules the incomplete callose wall is probably not the reason for the onset of apospory, but a sign of apospory. In *Tripsacum* sp. the restricted callose wall is also found and has been related to a disturbance in the normal meiotic process (Leblanc et al. 1995).

In *P. maximum*, nucellar cells which will develop into AIs are preferentially located in the chalazal part of the nucellus and are difficult to recognize at the ultrastructural level in an early stage of ovule development. After the arrest of sexual embryo sac development, a nucellar cell can redifferentiate to an AI. Cell size and nuclear and nucleolar size increase coincident with an increase in the number of vesicles and a small decrease in the density of ribosomes. Such change in the AI is comparable to the transition of a functional megaspore to the coenocytic stage (Willemse and van Went 1984). The AI cell-wall thickness remains 0.1 μm, which indicates cell-wall production to maintain the same thickness during cell enlargement. Multiple membranes were not observed in AI, possibly because no transition from sporophyte to gametophyte occurs.

The transition from an AI cell to the one-nucleate AE is characterized by the appearance of vacuoles situated at two cell poles and by an increase in cell size. The increase in ribosome density may reflect the increased need to assemble proteins necessary for further aposporic embryo sac development. The cell-wall thickness increases and plasmodesmatal connections diminish, leading to the end of symplastic transport and isolation of the cell.

In cases when only a sexual embryo sac develops, the nucellar cells retain their meristematic character around the MMC. The main differences between the functional megaspore and the AI are the lack of multiple membrane structures, later cell isolation by a thick cell wall and later expression of cell polarity expressed by the presence of storage products in the cell.

Reorganization of a nucellar cell that leads to an AE is comparable to the processes observed during initial cell differentiation that produce a nucellar or integumentary embryo. The last type of apomixis takes place at a

Fig. 7 Survey of the chalazal part of the nucellus with degenerating megaspores of the tetrad bordered by AIs. ×3600

Fig. 8 Part of an AI with numerous small vacuoles. ×16 000

Fig. 10 Cell wall of AI with a closed plasmodesma. Note the density of ribosomes. ×70 000

Fig. 11 Chalazal part of nucellus with degenerating sexual coenocytic embryo sac, a developing *AE, AI* and degenerating nucellar cells. ×3500

Fig. 12 Two AEs in one nucellus at different positions and developmental stages. AE_4 is four-nucleate and AE_1 is one-nucleate. ×160

Fig. 13 Isolated *Panicum*-type embryo sac with central cell, egg apparatus, but without antipodals. ×200

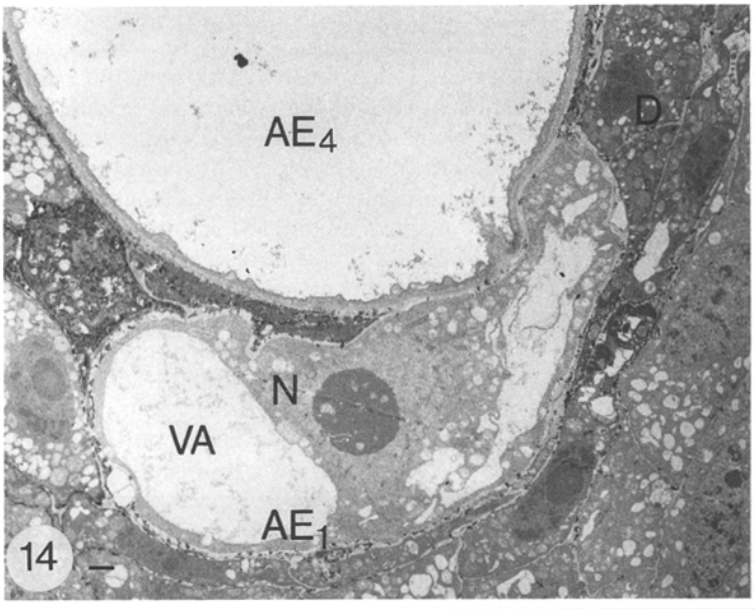
AE4
D
N
VA
AE1
14

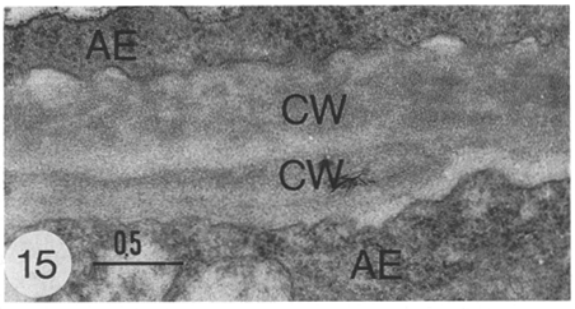
AE
CW
CW
0.5
15
AE

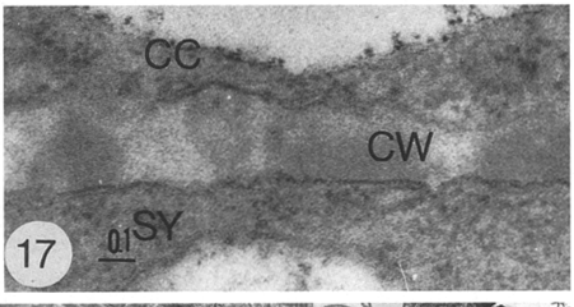
CC
CW
17
0.1
SY

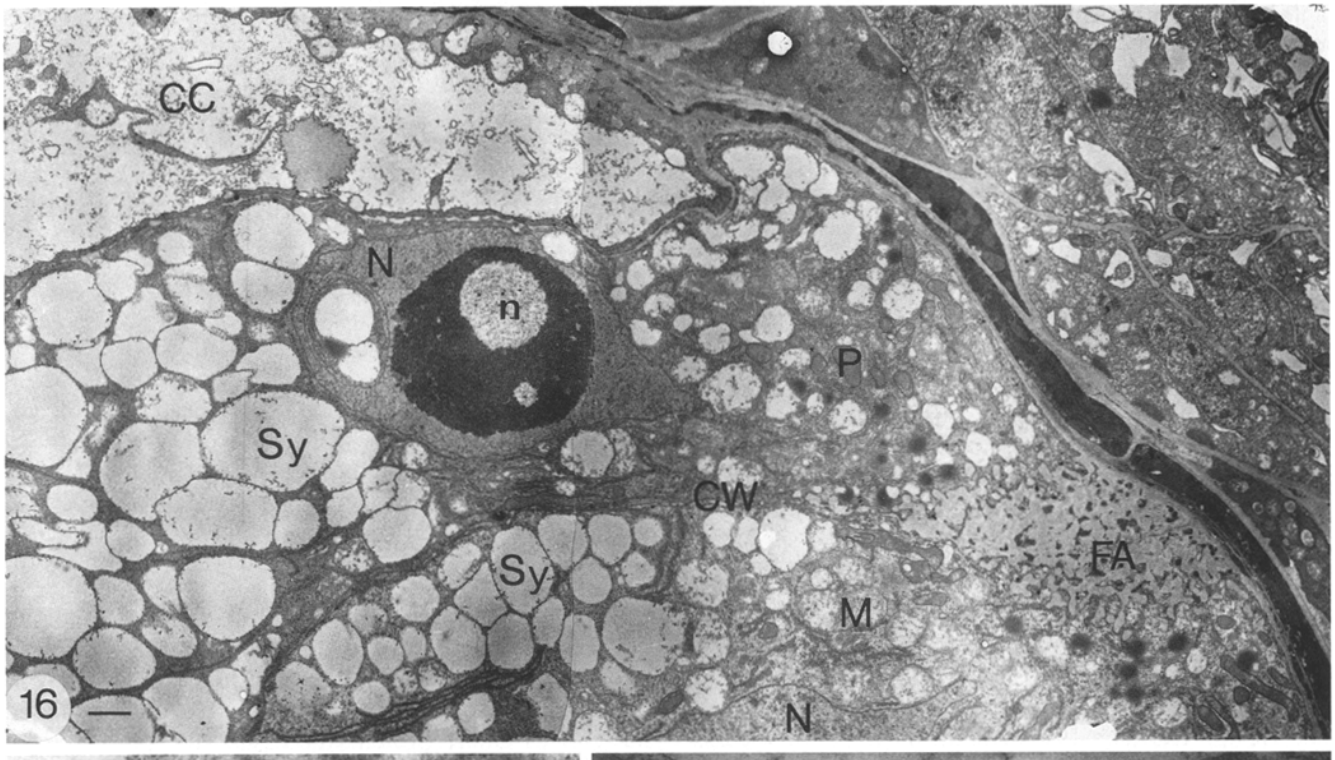
CC
N
n
P
Sy
CW
Sy
FA
M
16
N

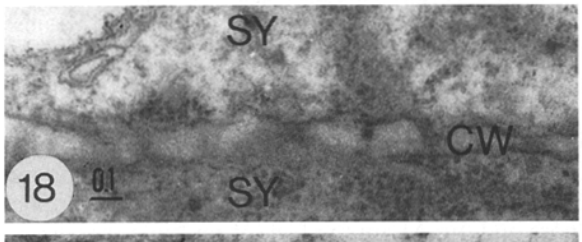
SY
CW
18
0.1
SY

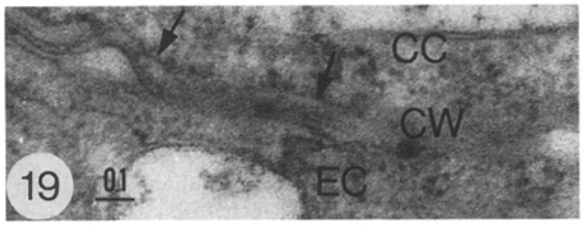
CC
CW
19
0.1
EC

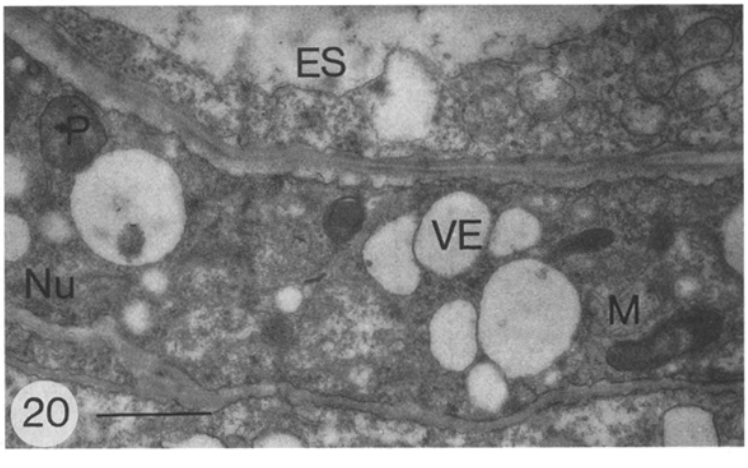
ES
P
VE
Nu
M
20

later stage of ovule development, when the sexual embryo sac is already formed. The nucellar cell initial of an adventive embryo is also marked by vacuolation and isolation by thickening of the cell wall and closure of plasmodesmata (Naumova and Willemse 1982; Naumova 1993). In apospory and in adventive embryony numerous nucellar cell initials can express their own genetic program that leads to an embryo sac or embryo, respectively. In the case of apospory the initiation starts in a very early stage of ovule development; adventive embryony initiation takes place in an ovule with a developed embryo sac.

Mature AE of the Panicum-type possess a normal egg apparatus. No differences can be observed between the cells of the egg apparatus, except for the presence of a filiform apparatus in the synergids. The observed thick micropylar cell wall between the synergids, that becomes a thin wall at the chalazal side is comparable to that observed on the egg apparatus of the apogametic *Trillium camschatcense* (Naumova 1991).

Pollen-tube penetration in one of the synergids and transfer of sperm cells are not observed. The observed local absence of a wall between synergid and egg cell in the chalazal part of the egg apparatus will not hamper sperm-cell transfer. According to the hypothesis of Savidan (1989), which postulates a complete egg cell wall, sperm-cell penetration cannot take place. However, in this study such a complete wall was not observed in the mature AE.

From this study it becomes clear that in a young nucellar cell at the structural level no signals of apospory can be detected. The earliest sign is the presence of a micropylar callose cap around the megameiocyte; later, the degeneration of dyad, tetrad or coenocytic embryo sac takes place. This early signal of the incomplete callose wall might include a preceding expression of an apomictic gene (Savidan 1982) or inducing factor (Nogler 1984) acting in the nucellar cells via the symplast and leading to an AI cell. The enlargement and vesiculation of the AI points to an uptake of water, with or without nutrients, from the nucellar environment. More apospores start to develop, while at the same time there is degeneration of the megaspores, coenocytic sexual embryo sac and nucellar cells. The development of the apospore needs a sufficient nutrient supply from the nucellus; this may be enhanced by degeneration of the megameiocytes or by the degeneration of dyads, tetrads, sexual coenocytic embryo sacs or nucellar cells. A role of a change in nutrition leading to apomixis, as reported by Bell (1992), should not be excluded at the onset of apospory in *P. maximum.*

Acknowledgements This research was funded by a Fellowship Grant from the International Agricultural Centre of the Netherlands and by the International Science Foundation of the U.S.A. We would like to thank Prof. A. Vassilyev (Russia) for fruitful discussions and Dr. J.H.N. Schel and Dr. Ir. R.W. den Outer for critical reading of the manuscript, Mr. S. Massalt and A.B. Haasdijk for the illustrations, and G. van Geerenstein (Unifarm) for the plant material.

Fig. 14 Detail of Fig. 12. Organized one-nucleate AE_1 at the chalazal side of the vacuolated AE_4. Note the degenerating nucellar cells. ×2500

Fig. 15 Detail of Fig. 14 showing the thick cell wall between two aposporous embryo sacs. Note the density of ribosomes. ×25 000

Fig. 16 Detail of synergids of AE. Note the more dense cytoplasm at the micropylar end near the filiform apparatus and at the chalazal end vesicles and small vacuoles. ×5000

Fig. 17 Detail of the cell wall between synergid and central cell near the micropyle. ×35 000

Fig. 18 Detail of the cell wall between the synergids near the micropyle below the filiform apparatus. ×35 000

Fig. 19 Detail of the very thin cell wall (*arrows*) between egg cell and central cell. ×40 000

Fig. 20 Lateral-chalazal part of sexual coenocyte embryo sac against a chalazal nucellar cell with dense cytoplasm. ×16 000

References

Abeln YS, Wilms HJ, van Wijk AJP (1985) Initiation of asexual seed production in Kentucky bluegrass, *Poa pratensis* L. In: Willemse MTM, Went JL van (eds) Proceedings of the 8th International Symposium on Sexual Plant Reproduction. Pudoc, Wageningen, pp 160–164

Battaglia E (1963) Apomixis. In: Maheswari P (ed) Recent advances in the embryology of angiosperms. University of Delhi, India, pp 221-264

Bell PR (1992) Apospory and apogamy: implications for understanding the plant live cycle. Int J Plant Sci 153:123–136

Brown WH, Emery WHP (1958) Apomixis in Gramineae. Tribe Andropogoneae. Bot Gaz 118:246–253

Carman JG, Grane CF, Riera-Lizarazu O (1991) Comparative histology of cell walls during meiotic and apomeiotic megasporogenesis in two hexaploid Australian *Elymus* species. Crop Sci 31:1527–1532

Dickinson HG (1981) Cytoplasmic differentiation during microsporogenesis in higher plants. Acta Soc Bot Pol 50:3–12

Dickinson HG, Heslop-Harrison J (1977) Ribosomes, membranes and organelles during meiosis in angiosperms. Philos Trans R Soc Lond B 277:327–342

Koltunow A (1993) Apomixis: embryo sac and embryo formation without meiosis and fertilization in ovules. Plant Cell 5:1425–1437

Leblanc O, Peel MD, Carman JG, Savidan Y (1995) Megasporogenesis and megagametogenesis in several *Tripsacum* species (Poaceae). Am J Bot 82:57–63

Naumova TN (1991) Apogamety in *Trillium canschatcense:* ultrastructural aspects. Apomixis News 3:16–17

Naumova TN (1993) Apomixis in angiosperms: nucellar and integumentary embryony. CRC press, Boca Raton, Fla

Naumova TN, Nijs APM den, Willemse MTM (1993) Quantitative analysis of aposporous parthenogenesis in *Poa pratensis* genotypes. Acta Bot Neerl 43:229–312

Naumova TN, Willemse MTM (1982) Nucellar polyembryony in *Sarcococca humilis*: ultrastructural aspects. Phytomorphology 32:94–108

Nogler GA (1984) Gametophytic apomixis. In: Johri BM (ed) Embryology of angiosperms. Springer, Berlin Heidelberg New York, pp 475–518

Russell SD (1979) Fine structure of megagametophyte development in *Zea mays*. Can J Bot 57:1093–1110

Rutishauser A (1969) Embryologie und Fortpflanzungsbiologie der Angiospermen. Springer, Berlin Heidelberg New York

Savidan JH (1982) Nature et hérédité de l'apomixis chez *Panicum maximum* Jacq. PhD thesis, Travaux et documents de O.R.S.T.O.M., Paris

Savidan JH (1989) Another "working hypothesis" for the control of parthenogenesis in *Panicum maximum*: the egg cell wall completion. Apomixis News 1:47–51

Schulz P, Jensen WA (1981) Pre-fertilization ovule development in *Capsella*: ultrastructure and ultracytochemical localization of acid phosphatase in the meiocyte. Protoplasma 107:27–45

Schulz P, Jensen WA (1986) Pre-fertilization ovule development in *Capsella*: the dyad, tetrad, developing megaspore, and two-nucleate gametophyte. Can J Bot 64:875–884

Warmke HE (1954) Apomixis in *Panicum maximum*. Am J Bot 41:5–11

Willemse MTM, Went JL van (1984) The female gametophyte. In: Johri BM (ed) Embryology of angiosperms. Springer, Berlin Heidelberg New York, pp 159–196